

## Site-Specific Functionalization of Anisotropic Nanoparticles: From Colloidal Atoms to Colloidal Molecules

Fan Li, Won Cheol Yoo, Molly B. Beernink, and Andreas Stein\*

Department of Chemistry, University of Minnesota, 207 Pleasant Street SE,  
Minneapolis, Minnesota 55455

Received October 1, 2009; E-mail: a-stein@umn.edu

**Abstract:** Multipodal nanoparticles (NPs) with controlled tethers are promising principal building blocks, useful for constructing more complex materials, much like atoms are connected into more complex molecules. Here we report colloidal sphere templating as a viable means to create tetrapodal NPs with site-specific tethers. Amorphous sol–gel materials were molded by the template into shaped NPs that mimic tetravalent atoms but on the length scale of colloids. Synthetic methods were developed to modify only the tips of the tetrapods with a range of possible functional groups to generate anisotropic NPs capable of directional bonding to other NPs. We also illustrate that sets of tethered “colloidal atoms” can assemble themselves into “colloidal molecules” with precise placement of the modifying colloids. The templating and tethering approaches to these anisotropic colloidal building blocks and the assembly methods are applicable to many compositions regardless of crystal structure, therefore lending themselves to the fabrication of complex assemblies, analogous to those found in the molecular regime.

### Introduction

Self-assembly processes could benefit substantially from nanoparticles (NPs) with anisotropic structures and functions.<sup>1</sup> Such particles, as building blocks, are capable of establishing directional interactions<sup>2</sup> and thereby facilitate either self-assembly or guided assembly into structures with different dimensionalities,<sup>1</sup> ranging from functional multicomponent clusters to extended arrays with desired symmetries.<sup>3</sup> The variety of particles with different shapes, sizes, and compositions reported in the literature has been categorized based on geometry and connectivity.<sup>1</sup> In this regard, each group of NPs could be considered as a type of principal building block, and the design and synthesis of complex superstructures could, in principle, be realized by choosing from a few building blocks with simple geometries. This approach has been compared to organic synthesis, where a vast number of distinct compounds are synthesized from just a few types of atoms (e.g., C, H, O, and N) that influence the product structure through directional bonding.<sup>4</sup> Similarly, one can envision great advances in the self-assembly of materials following purposely designed trajectories, if atom-like principal building blocks with colloidal dimensions become readily available.

The shapes of multipodal nanoparticles and their possible directional interactions have been compared to valences of atoms, i.e., the number of bonds that the atoms can form in various directions.<sup>5</sup> The decoration of podal ends with functional groups and subsequent bonding with other nanoparticles would lead to true resemblances of atoms and molecules but now at

the colloidal or nanoscale.<sup>6–8</sup> Theoretical studies have predicted that suitably designed anisotropic particles with tethers are capable of self-assembling into some highly coveted structures.<sup>9,10</sup> Experimentally, one recent example extending the valence bond concept to nanoparticles is found in CdSe quantum dots with tetrapodal structures,<sup>11</sup> which were tethered with Au via selective reduction, thereby forming a structure analogous to atoms with  $sp^3$  hybrid orbitals.<sup>7</sup> Very recently, these tethered quantum dots were observed to form an extended network, as a first step toward their controlled assembly.<sup>12</sup> However, structural control through nanocrystal engineering, though under rapid development,<sup>13</sup> is limited to a small group of crystalline materials, and the tethering mechanism is also quite unique. One might, therefore, desire a more general shaping strategy that is not tied to a specific material, as well as more flexible tethering methods that enable “reactions” of “colloidal atoms” to form “colloidal molecules”.<sup>2,8,14</sup>

Here, we used colloidal templates as molds to shape sol–gel-based multipodal nanoparticles with site-selective tethering capable of directional interactions. Colloidal spheres as templates

(1) Glotzer, S. C.; Solomon, M. J. *Nat. Mater.* **2007**, *6*, 557–562.  
 (2) Nelson, E. C.; Braun, P. V. *Science* **2007**, *318*, 924–925.  
 (3) van Blaaderen, A. *Nature* **2006**, *439*, 545–546.  
 (4) Nelson, D. R. *Nano Lett.* **2002**, *2*, 1125–1129.  
 (5) Jang, J. H.; Ullal, C. K.; Kooi, S. E.; Koh, C.; Thomas, E. L. *Nano Lett.* **2007**, *7*, 647–651.

(6) Liu, H.; Alivisatos, A. P. *Nano Lett.* **2004**, *4*, 2397–2401.  
 (7) Mokari, T.; Rothenberg, E.; Popov, I.; Costi, R.; Banin, U. *Science* **2004**, *304*, 1787–1790.  
 (8) Glotzer, S. C. *Science* **2004**, *306*, 419–420.  
 (9) Zhang, Z.; Keys, A. S.; Chen, T.; Glotzer, S. C. *Langmuir* **2005**, *21*, 11547–11551.  
 (10) Glotzer, S. C.; Horsch, M. A.; Iacovella, C. R.; Zhang, Z.; Chan, E. R.; Zhang, X. *Curr. Opin. Colloid Interface Sci.* **2005**, *10*, 287–295.  
 (11) Milliron, D. J.; Hughes, S. M.; Cui, Y.; Manna, L.; Li, J.; Wang, L. W.; Alivisatos, A. P. *Nature* **2004**, *430*, 190–195.  
 (12) Figuerola, A.; Franchini, I. R.; Fiore, A.; Mastria, R.; Falqui, A.; Bertoni, G.; Bals, S.; Van Tendello, G.; Kudera, S.; Cingolani, R.; Manna, L. *Adv. Mater.* **2009**, *21*, 550–554.  
 (13) Xia, Y.; Xiong, Y.; Lim, B.; Skrabalak, S. E. *Angew. Chem., Int. Ed.* **2009**, *48*, 60–103.  
 (14) Grill, L.; Dyer, M.; Lafferentz, L.; Persson, M.; Peters, M. V.; Hecht, S. *Nat. Nanotechnol.* **2007**, *2*, 687–691.



**Figure 1.** Schematic diagrams illustrating the processing steps to produce end-functionalized tetrapods.

can be readily synthesized from different materials, and methods of packing spherical or quasispherical colloids into colloidal clusters (oligomers) and colloidal crystals have been widely studied, where the assembly is usually based on *nondirectional* interactions, such as van der Waals forces and electrostatic forces,<sup>15,16</sup> or subject to external fields, such as phase boundaries,<sup>17,18</sup> electromagnetic fields,<sup>19</sup> and confinement effects.<sup>20,21</sup> Using close-packed colloidal crystals as templates, we synthesized more interesting, tetrapodal particles which mimic hybrid orbitals with tetrapodal ( $sp^3$ ) configurations (Figure 1). The podal ends were selectively tethered with functional groups, thereby granting them the capability of site-specific *directional* bonding, as exemplified by coupling via thiol–gold interactions or by reductive amination between tethered nanoparticles. The synthetic strategies were designed from a nanoengineering perspective, and the particles were prepared by sol–gel chemistry, providing a methodology suitable for a wide range of materials.

## Experimental Section

Descriptions of the materials, the synthesis of the polymer sphere templates, and characterization methods are provided in the Supporting Information.

**Three-Dimensionally Ordered Macroporous (3DOM) Silica Synthesis and Surface Passivation.** A 3DOM silica structure was first prepared by templating against polymethyl methacrylate (PMMA) colloidal crystals of face-centered cubic symmetry. Centimeter-sized colloidal crystal templates were half-immersed in a silica sol–gel precursor [2 g of tetraethyl orthosilicate (TEOS) and 1 g of HCl (1M)], which was driven into the interstices within the colloidal crystals by capillary forces. After complete infiltration, the sol–gel/colloidal crystal composites were stored in a closed container at 50 °C for 48 h. The PMMA spheres were removed by dissolution in toluene, and the resulting 3DOM silica was harvested by filtration and dried in air.

3DOM silica powder was then redispersed in dry toluene and surface functionalized with passivation groups by reacting with a range of alkoxy silanes bearing different side chains (see the Results and Discussion). In a typical synthesis, 0.23 g of silane and 0.1 g of 3DOM silica were mixed in 60 mL of dry toluene and reacted at 60 °C with 0.011 g of *p*-toluenesulfonic acid (PTSA) as the catalyst and under  $N_2$  protection. The functionalized silica structures were collected by filtration and repeatedly washed with fresh toluene. To ensure complete passivation, the surface functionalization and washing steps were repeated twice to increase the silane coverage on the silica surface. Next, the silica particles were dispersed in PTSA-saturated toluene and heated at 90 °C for 48 h under a  $N_2$  purge.

**Tetrapod Synthesis and Foot-Functionalization.** Tetrapodal structures were obtained through disassembly of the 3DOM structure. For disassembly and tethering, 0.1 g of 3-mercaptopropyltrimethoxy silane (MPTMS) and 0.02 g of 3DOM silica were mixed in toluene and stirred vigorously for 48 h. The shearing force induced by stirring fractured the structures into tetrapods and cubes, and the MPTMS was simultaneously grafted onto the freshly generated podal tips. Alternatively, ultrasonication could be applied for the disassembly of 3DOM silica, which, however, usually resulted in slightly less regular particles. To enrich the tetrapods from the mixture, a gradient solution of ethylene glycol (EG) and EG/EtOH (50:50 wt:wt) was prepared in a two-jar gradient solution apparatus. The mixture of particles was dispersed in EtOH, loaded on top of the gradient solution, and centrifuged at 1000 rpm for 30 s. Only the top 1/3 layer was collected, and the particles were redispersed in EtOH. The centrifugation process was then repeated 3–5 times. Typical batches yielded ca. 2 mg of fractionated particles (about 70% tetrapods), corresponding to approximately  $10^{13}$  particles, i.e., sufficient for subsequent investigations of assembly.

**Au Tethering.** For tethering of Au NPs, 300  $\mu$ L of a toluene dispersion of silica multipodal particles (ca. 3 wt %) was mixed with a 150  $\mu$ L toluene dispersion containing Au NPs (either 1–2 nm or ca.  $3.2 \pm 0.5$  nm in diameter), followed by the addition of another 500  $\mu$ L of dry toluene. The mixture was stirred at room temperature for 2.5 h, and then the particle assemblies were collected by centrifugation and washed three times each with PTSA-saturated toluene and dry toluene.

**Colloidal Silica Tethering.** To attach colloidal silica spheres, the same tethering procedure was applied on the multipodal particles as described before, except that triethoxysilylundecanal was used as the tethering agent. Meanwhile, 2 mg of 45 nm silica spheres were surface functionalized by mixing them with 50 mg of 3-aminopropyltrimethoxy silane (APDMES) in 1 mL of EtOH and stirring for 24 h, followed by repeated washing with EtOH. Afterward, ca. 2 mg of triethoxysilylundecanal-tethered multipodal nanoparticles in 500  $\mu$ L of toluene were mixed with 1 mg of silica spheres in 500  $\mu$ L of EtOH, followed by the addition of 0.5 mg of  $NaBH_4(OAc)_3$  and incubation for 24 h. The sample was finally isolated by centrifugation.

**Joint Assembly by SH-Tethered (HS- $T_d$ ) and Au-Tethered (Au- $T_d$ ) Tetrapods.** Toluene dispersions containing 1–5 wt % of HS- $T_d$  and Au- $T_d$ , respectively, were prepared. They were set aside for 30 min to allow any excessively large particles to sediment. Afterward, equal amounts of the supernatants were mixed in a 1.5 mL cuvette and stirred with a pipet to facilitate mixing. The cuvette was then incubated at different temperatures to observe phenomena related to self-assembly.

## Results and Discussion

The typical products obtained during the shaping and tethering procedures for the multipodal NPs are summarized in Figure 2. Slow sedimentation of monodisperse PMMA colloids in  $H_2O$  formed close-packed arrays with face-centered cubic (fcc) symmetry (Figure 2a).<sup>20</sup> By templating against highly ordered PMMA colloidal crystal templates, 3D macroporous silica structures were obtained, which inherited the ordering and symmetries from the template structures (Figure 2b).<sup>22</sup> The

- (15) Kalsin, A. M.; Fialkowski, M.; Paszewski, M.; Smoukov, S. K.; Bishop, K. J. M.; Grzybowski, B. A. *Science* **2006**, *312*, 420–424.  
 (16) Hiramoto, H.; Osterloh, F. E. *Langmuir* **2003**, *19*, 7003–7011.  
 (17) Manoharan, V. N.; Elsesser, M. T.; Pine, D. J. *Science* **2003**, *301*, 483–487.  
 (18) Subramaniam, A. B.; Abkarian, M.; Stone, H. A. *Nat. Mater.* **2005**, *4*, 553–556.  
 (19) Sawetzki, T.; Rahmouni, S.; Bechinger, C.; Marr, D. W. M. *Proc. Natl. Acad. Sci. U.S.A.* **2008**, *105*, 20141–20145.  
 (20) Yin, Y.; Xia, Y. *Adv. Mater.* **2001**, *13*, 267–271.  
 (21) Ozin, G. A.; Yang, S. M. *Adv. Funct. Mater.* **2001**, *11*, 95–104.

- (22) Holland, B. T.; Blanford, C.; Stein, A. *Science* **1998**, *281*, 538–540.

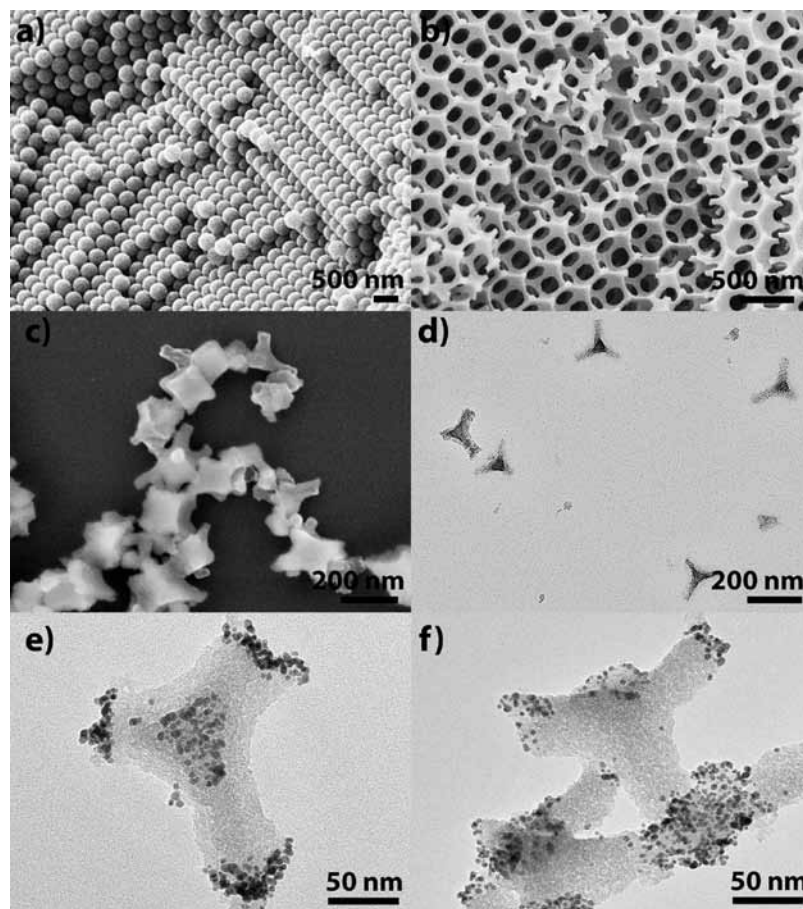


**Figure 2.** Electron microscopy images illustrating materials obtained at various stages during the synthesis procedures. (a) SEM image of a PMMA colloidal crystal. (b) 3DOM silica prepared by replicating the interstitial space in the colloidal crystal template. (c) A mixture of silica tetrapods and cubes after the disassembly. (d) TEM image of functionalized tetrapods enriched from the mixture. (e) A zoomed-in image showing a tetrapod with Au tethers. (f) TEM image illustrating the tendency for aggregation between Au-tethered tetrapodal particles.

original colloidal crystals with fcc symmetry contain two types of interstitial spaces corresponding to tetrahedral and octahedral holes in the fcc sphere array, and therefore the 3DOM structure could be considered to be composed of interconnected tetrahedra (67%) and cubes (33%).<sup>23,24</sup> Multipodal particles were then derived by disassembling these structures as illustrated in Figure 1. Figure 2c shows a mixture of disassembled particles, which can be easily recognized as the “broken pieces”, or “building blocks” of the original 3DOM structure. A broader survey of the disassembly product can be found in Figure S2. Typically, the fractured structures include 70–80% individual primary building blocks, as well as dimers or larger superstructures, from which the smaller tetrahedra were harvested by density gradient centrifugation (Figure 2d). It should be emphasized that the particles obtained after disassembly can be very uniform in size and shape;<sup>24</sup> for example, the cubes have been found to assemble into extended regions of simple cubic packing.<sup>25</sup> In contrast to our previous study, where disassembly was induced by stresses during the calcination of 3DOM silica with hierarchical pore structure,<sup>24</sup> shear was used to effect disassembly<sup>23</sup> in this work

to permit passivation of the macropore surface and to maintain the surface groups during and after disassembly.

Surface passivation of 3DOM silica prior to disassembly of the macrostructure eliminated most surface silanol groups. Site-specific functionalization with tethering groups was then possible on the freshly exposed podal ends after disassembly. Ideally, such passivation may be realized by coating a thin layer of inert molecules on the macropore walls. As the passivation layer had to survive the disassembly process, which involved considerable mechanical agitation, chemical grafting was preferred over physical deposition. In the current study, the surface silanol groups could be replaced by reacting with alkoxysilane, and we performed a series of experiments with different silanes as passivating reagents, which will be discussed in the following paragraphs. Subsequently, mechanical agitation (stirring) or ultrasonication was applied to rupture the connections between vertices in the structures, leading to individual building blocks. The podal ends of the particles were populated with silanol groups, either pre-existing in the silicate structure or newly formed during the fracturing process,<sup>26</sup> that could then be modified with a tethering agent (Table 1). In practice this was realized through a simultaneous disassembly and functionalization process. To visualize the site-specific functionalization,

(23) Li, F.; Xu, L.; Zhou, W. L.; He, J.; Baughman, R. H.; Zakhidov, A. A.; Wiley, J. B. *Adv. Mater.* **2002**, *14*, 1528–1531.

(24) Li, F.; Wang, Z.; Stein, A. *Angew. Chem., Int. Ed.* **2007**, *46*, 1885–1888.

(25) Li, F.; Delo, S. A.; Stein, A. *Angew. Chem., Int. Ed.* **2007**, *46*, 6666–6669.

(26) D’Souza, A. S.; Pantano, C. G. *J. Am. Ceram. Soc.* **1999**, *82*, 1289–1293.



**Table 1.** Passivation and Tethering Agents

Passivation agents	Tethering agents
$\text{CH}_3(\text{CH}_2)_{14}\text{CH}_2\text{-Si-(OCH}_3)_3$ or $\text{CH}_3\text{O}(\text{CH}_2\text{CH}_2\text{O})_{6-9}(\text{CH}_2)_3\text{-Si-(OCH}_3)_3$	$\text{HS-(CH}_2)_3\text{-Si-(OCH}_3)_3$ $\text{CHO-(CH}_2)_{10}\text{-Si-(OCH}_3)_3$ $\text{H}_2\text{N-(CH}_2)_3\text{-Si(CH}_3)_2\text{-OCH}_2\text{CH}_3$

MPTMS was used as a tethering reagent and gold NPs as a contrast agent. The distribution of active functional groups and passivating groups can thus be examined by chemical adsorption of Au NPs (either 1–2 or 3 nm average Au diameter) on the thiolated surfaces.

Searching for a suitable passivation reagent, we initially examined phenyl trimethoxysilane, because treatment with aromatic organosilane, as often used in the silylation of glassware, could significantly alter the properties of the silica surface. However, passivation proved to be incomplete when MPTMS was subsequently grafted and Au clusters with diameters of 1–2 nm were attached (Figure 3, left panel). This could be due to the fact that the bulky phenyl groups prevented the consumption of all the surface silanol groups and some residual silanol was still available for the following MPTMS grafting.<sup>27</sup> On the other hand, when methyltrimethoxysilane (MTMS) was used, complete passivation could be achieved, but meanwhile the podal ends also lost their activity for Au tethers (Figure 3, right panel). In this case, MTMS with its smaller methyl group permitted the formation of a close-packed monolayer binding all the surface silanols.<sup>27</sup> However, since the 3DOM structures were made through a sol–gel process, where internal porosity was a common feature, the small MTMS molecules may have also coated micropores or small mesopores in the structure, and thereby caused “internal overpassivation”, which led to the inactive tips after the disassembly. Internal overpassivation would be even more pronounced if templated mesopores were present as in our earlier report of particle synthesis by disassembly.<sup>24</sup> A surfactant template for mesopores was therefore not used here, even though additional mesopores would weaken the interconnects between tetrahedral and octahedral hole replicates and would facilitate disassembly.

Therefore, it may be concluded that two criteria existed for picking a suitable passivating reagent in order to successfully implement this synthetic strategy. The passivating reagent should be able to completely cover the 3DOM structure externally and render it inert to the following tethering reagent. In addition, the passivating reagent should be prevented from reaching internal pores. For the best results, trimethoxysilanes containing two types of long-chain structures were selected: 2-[methoxy-(polyethyleneoxy)propyl]trimethoxy silane (PEO-silane), a siliceous passivating reagent for biotechnology,<sup>28</sup> and *n*-hexadecyltrimethoxy silane (C<sub>16</sub>-silane) (Table 1). The long-chain structures provided additional protection against any nonspecific adsorption and also prevented them from entering internal micropores. Furthermore, the PEO- and C<sub>16</sub>-silane coating could furnish particles with dissimilar surface polarities, which may facilitate the future application of these particles in different

media. After a single passivation step with PEO-silane or C<sub>16</sub>-silane, it was found that although small Au NPs (1–2 nm) no longer attached themselves to the protected surface, larger Au NPs (3 nm) were still adsorbed throughout the structure (Figure 3, middle panel). Although polyethylene oxide/alkyl chains eliminated surface silanols only partially in a single passivation step, with extended lengths up to 3.1 nm<sup>28</sup> they could effectively repel small Au clusters and prevent them from reaching the embedded thiol groups (Figure 3). Such repulsion became less effective for larger Au clusters, perhaps because these extended over larger areas and could penetrate the surface layer and bind with the underlying thiol groups. To realize true passivation, a highly condensed layer was needed to form a strong network and more completely eliminate surface silanol groups.<sup>27</sup> This was achieved by a two-step reaction as depicted in Figure 4: the passivating reagent (silane) was first anchored to the surface of the porous silica in toluene at 60 °C, with PTSA as the catalyst. This grafting process was repeated multiple times to increase the amount of attached silane. Afterward, the silica was redispersed in PTSA-saturated toluene at 90 °C to enhance lateral condensation of silane groups. The improved condensation was evident from an increase in the ratio of T<sup>3</sup>:T<sup>2</sup> resonances in solid-state NMR spectra (i.e., resonances corresponding to organosilane groups without and with a remaining hydroxyl group, Figure S3), and it was critical to achieve complete passivation. After this optimal passivation process, almost 100% site-selectivity could be realized when the tethering process was conducted. As shown in Figure 2e and 2f and Figure 3, middle panel, the Au NPs packed densely on the podal ends, whereas almost no Au NPs were visible on the surrounding podal walls, indicating highly selective functionalization. It should be noted that those building blocks originally located on the edge or surface of the original 3DOM network contained podal ends that were exposed during the passivation process with PEO. The corresponding multipods obtained after disassembly contained fewer active vertices. The number of these particles with “lower valence”<sup>6</sup> could be increased intentionally by partially fracturing the 3DOM structures prior to passivation (Figure 5).

An ultimate goal of this research is to connect the anisotropic building blocks into extended and, ideally, periodic structures, for example, the highly desirable diamond photonic crystal structure. Here, the facile synthesis and tethering process provided a platform for us to explore the self-assembly behavior of multipodal building blocks. Numerous silanes bearing different functional groups are available as potential tethers and can be attached in the same manner as MPTMS, i.e., through anchoring with surface silanol groups. Alternatively, the attached Au NPs can serve as anchors for thiolated DNA<sup>29,30</sup> or other functionalized nanoobjects.<sup>31,32</sup> We have explored both strategies to form “colloidal molecules” and potentially “colloidal macromolecules” as presented in the following paragraphs.

To demonstrate the self-assembly of colloidal molecules, the functionalized multipodal nanoparticles and colloidal silica spheres were used as building blocks. In the series of multipodal structures, the tetrapodal particles are most interesting for constructing 3D periodic nanostructures. Therefore, the study

(27) Wirth, M. J.; Fairbank, R. W. P.; Fatunmbi, H. O. *Science* **1997**, *275*, 44–47.

(28) Papra, A.; Gadegaard, N.; Larsen, N. B. *Langmuir* **2001**, *17*, 1457–1460.

(29) Alivisatos, A. P.; Johnsson, K. P.; Peng, X.; Wilson, T. E.; Loweth, C. J.; Bruchez, M. P., Jr.; Schultz, P. G. *Nature* **1996**, *382*, 609–611.

(30) Mirkin, C. A.; Letsinger, R. L.; Mucic, R. C.; Storhoff, J. J. *Nature* **1996**, *382*, 607–609.

(31) Galow, T. H.; Boal, A. K.; Rotello, V. M. *Adv. Mater.* **2000**, *12*, 576–579.

(32) Shipway, A. N.; Lahav, M.; Gabai, R.; Willner, I. *Langmuir* **2000**, *16*, 8789–8795.

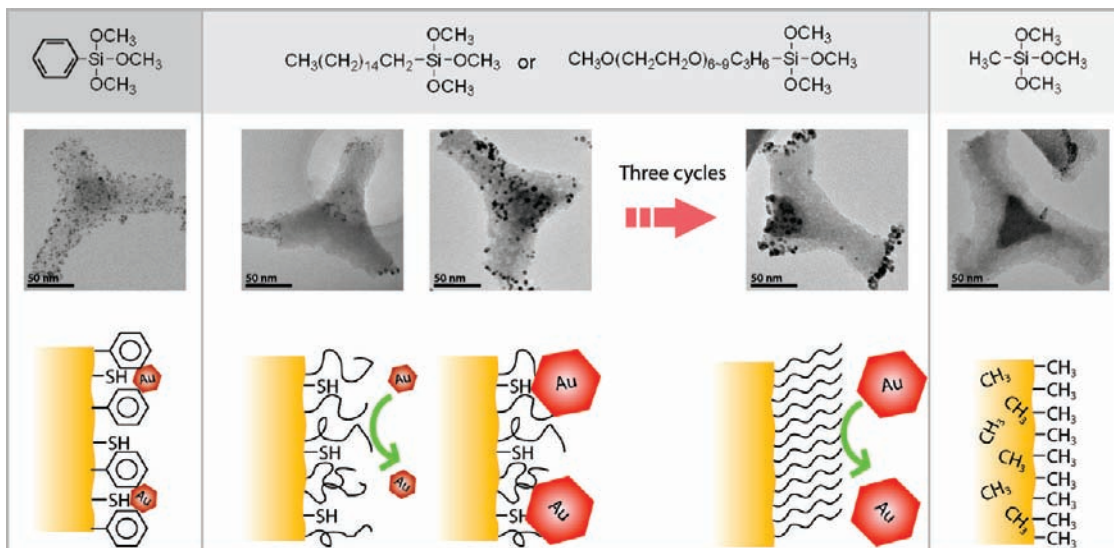


**Figure 3.** Summary of surface functionalization with different passivating agents. Left: Passivation with phenyltrimethoxysilane results in nonspecific adsorption of gold particles. Middle: The listed passivating agents with long alkyl chains provide site specific adsorption after multiple passivation steps. Right: No gold particle adsorption occurs for a control sample that was fully passivated with methyltrimethoxysilane.

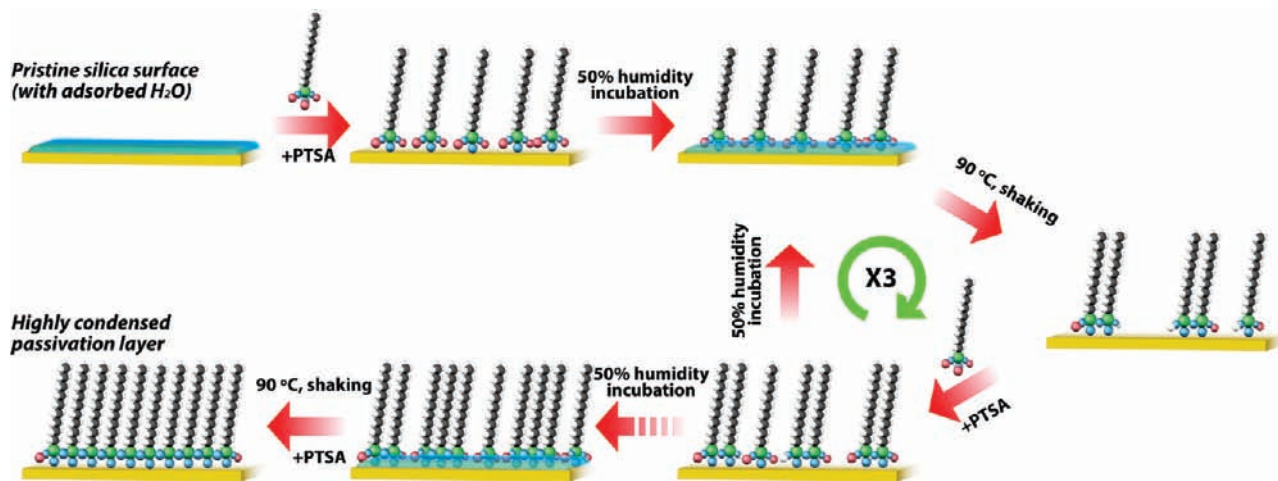
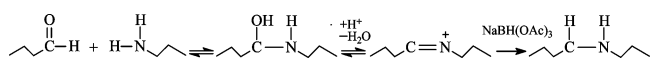


**Figure 4.** Schematic diagram of the passivation process. The procedure includes multiple grafting and surface rehydroxylation steps and a final condensation step.

of particle assembly was focused on tetrapodal particles, but it should be straightforward to extend the protocol to other particles. Many approaches exist for specific binding between binary NPs, ranging from chemical reaction or electrostatic attraction to more complicated DNA hybridization. Here, tetrapodal particles tethered with triethoxysilylundecanal (Figure 6a) were mixed with aminated colloidal silica spheres ca. 45 nm in diameter (Figure 6b),<sup>33</sup> and the mixture was incubated in the presence of  $\text{NaBH}(\text{OAc})_3$ . During this process, reductive amination occurred, and colloidal spheres were immobilized on the podal ends.



As shown in Figures 6c, S4, and S5, silica colloids were accurately mounted on the podal tips with dimensions less than 20 nm; meanwhile, no random adsorption on other regions was observed. Multiple colloidal silica spheres could be mounted

onto one tetrapod, thereby forming an ammonia-like, colloidal molecule (Figure 6d–f). The precision and selectivity of this assembly process clearly demonstrates the advantage of building blocks with both structural and functional anisotropies. The process can thus be considered as a “chemical reaction” between different colloidal atoms to form colloidal molecules. Moreover, one may choose suitable functional groups and design a sequential route, much like a synthetic organic chemist, to fabricate more complex structures.

Our second strategy was based on the assembly of multipods with existing Au tethers, which were still active toward approaching SH groups, as tested by a thiolated Texas-red dye (Figure S6). The tendency of Au–thiol attraction to drive particle assembly was first observed in preparing Au-tethered tetrapods when insufficient Au sol was added in the mixture

(33) Fan, W.; Snyder, M. A.; Kumar, S.; Lee, P. S.; Yoo, W. C.; McCormick, A. V.; Lee Penn, R.; Stein, A.; Tsapatsis, M. *Nat. Mater.* **2008**, *7*, 984–991.



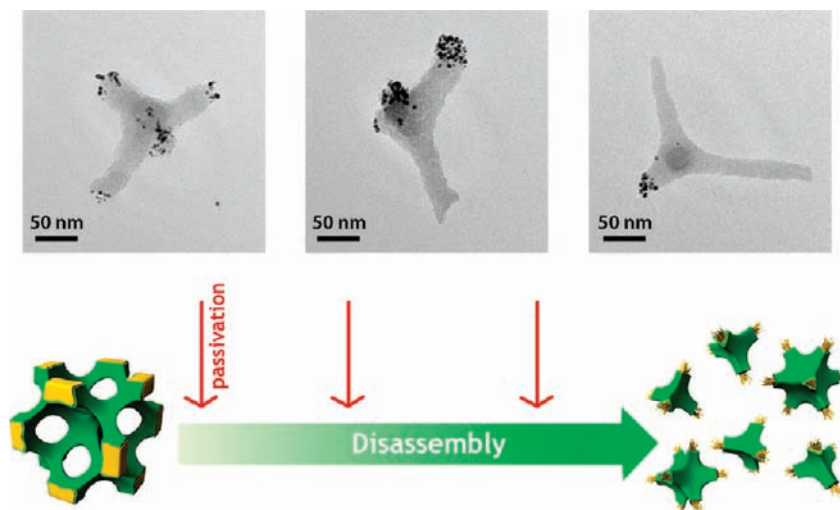


**Figure 5.** Schematic diagram showing the relationship between the scheduling of the passivation process and the average number of tethered feet on the tetrapods. Passivation performed before disassembly produced tetrapods with all of four feet active for tethering. Passivation on partially disassembled structures resulted in tetrapods with fewer active feet (on the average), as some pod ends were already exposed to passivating groups. The average number of less active feet could be increased intentionally by partially fracturing the 3DOM structures prior to passivation.

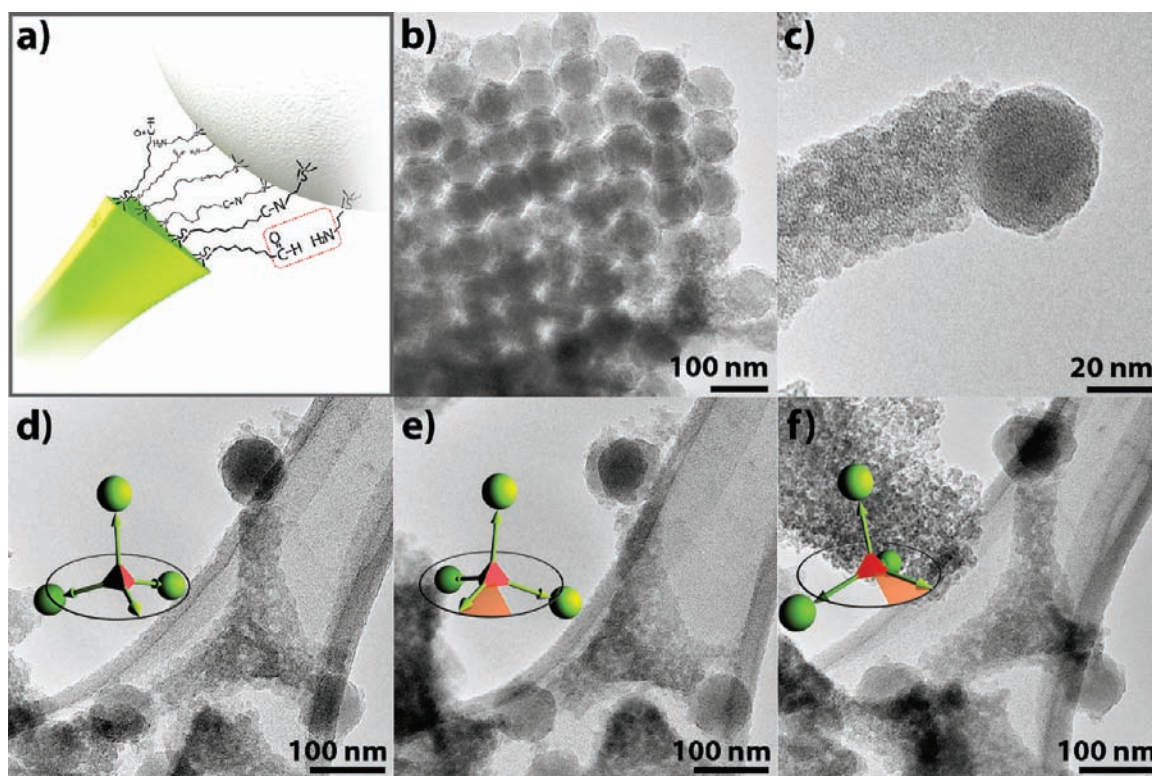


**Figure 6.** From colloidal atoms to colloidal molecules: site-specific assembly of colloidal silica spheres on tethered tetrapods. (a) Schematic of the assembly process based on reductive amination. (b) Monodisperse silica colloidal spheres, ca. 45 nm in diameter, prepared by a seed growth method. (c) TEM image showing a silica colloid mounted on a podal end. (d) TEM image showing an ammonia-like nanostructure formed by three spherical silica colloids attached to one tetrapod. (e and f) The same region under the TEM with  $\pm 25^\circ$  tilting. The models drawn in panels d, e, and f are intended as guides to indicate the viewing angle and the 3D structure of the colloidal molecule.

(Figure 2f). We herein adopted a simple scheme of Au-mediated assembly and analyzed the interactions between Au-tethered tetrapods and thiolated ones (Figure 7a). Although separate, both particle dispersions remained stable for several days and flocculation occurred immediately upon mixing and led to a woolly suspension. This, as we propose, was due to the specific interactions between thiolated podal ends and Au-tethered podal

ends, and the attraction between the multivalent particles eventually resulted in a 3D network on a macroscopic scale. The vital role of Au tethers as intermediates was further proved by the observation that adding free Au NPs into the mixture greatly suppressed the flocculation, as free Au NPs could more readily capture unsaturated SH surface groups compared to Au tethers already bound to another multipod. The freshly flocc-

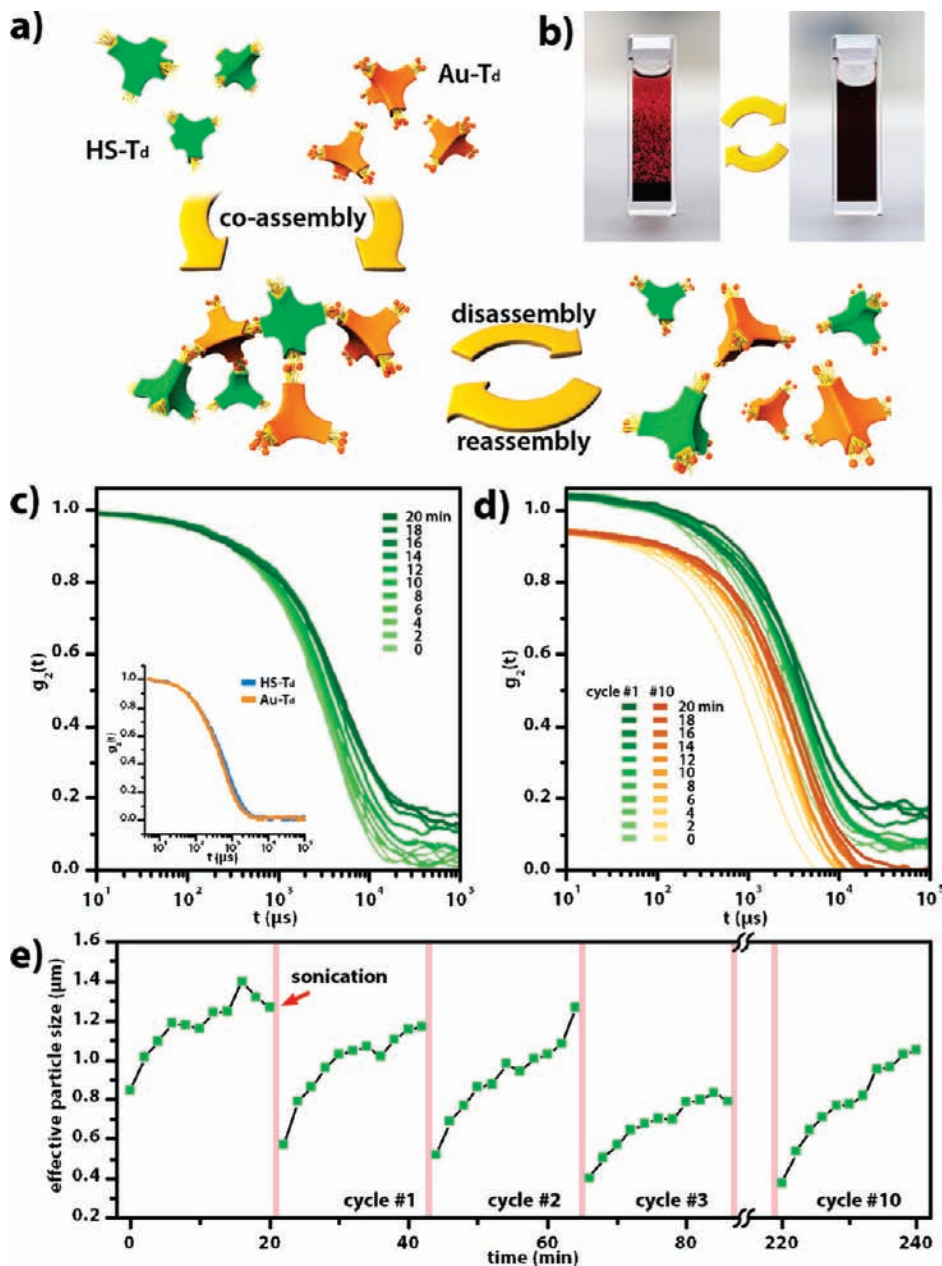


**Figure 7.** Reversible assembly/disassembly processes by mercapto-tethered tetrapods (HS-T<sub>d</sub>) and Au-tethered tetrapods (Au-T<sub>d</sub>). (a) Schematic diagram showing how a mixture of HS-T<sub>d</sub> and Au-T<sub>d</sub> colloids may assemble into 3D-interconnected macroscopic structures. (b) Photographs of a cuvette containing a mixture of HS-T<sub>d</sub> and Au-T<sub>d</sub> in toluene in the aggregated (left) and dispersed (right) states. The inset shows data for the two dispersions before mixing, and neither of the two dispersions undergo significant size changes in 20 min (Figure S12). (c) Normalized correlation functions from DLS measurements following the initial mixing process. The inset shows data for the two dispersions before mixing, and neither of the two dispersions undergo significant size changes in 20 min (Figure S12). (d) Comparison of the evolution of the correlation function in the first reassembly process (cycle #1) and the tenth reassembly (cycle #10). The curves are offset by  $\pm 0.05$  for cycle #1 and #10, respectively. (e) Effective particle size change during the mixing and 10 cycles obtained from the DLS data. Note that secondary peaks in some  $g_2(t)$  curves are associated with a minimal amount of much larger aggregates,<sup>34</sup> whose formation is not likely related to the site-specific assembly.<sup>35</sup> These peaks were cut off in fitting average particle size.

culated material could, however, be reverted to a clear appearance with gentle shaking (Figure 7b), after which flocculation resumed. This indicates that the system was governed by weak interactions, possibly in a dynamic state with constant assembly and disassembly of particles. Therefore, instead of capturing a definite microstructure, we used dynamic light scattering (DLS) to further study the dynamics of the assembly process. To be suitable for DLS measurements, the particle suspensions were diluted 5-fold with ethanol. Both the thiolated tetrapods and the Au-tethered tetrapods displayed steady hydrodynamic particle sizes around 150 nm, which roughly corresponds to

dimensions of single particles measured by TEM. Upon mixing, the fitted average particle size abruptly changed to ca. 850 nm, indicating that a certain degree of aggregation had occurred. Further aggregation was reflected by the shifts and slope changes of the time intensity autocorrelation functions ( $g_2(t)$ ), which indicate greater correlation between tetrapods as these formed larger clusters with a broader size distribution. After 20 min, the initial aggregate was redispersed with stirring and another DLS measurement was performed. This sedimentation/redispersion process was cycled 10 times, and very similar patterns of the  $g_2(t)$  and particle size evolution were observed (Figure

7c–e), indicating that the assembly process became slower but was fully reversible. The reversibility of the assembly may benefit in situ studies of the tetrapod assembly process, by allowing tests of different parameters with only one sample. A more detailed analysis of the assembly process is currently ongoing.

## Conclusions

We have shown a general and flexible colloidal templating approach toward tetrapodal nanoparticles and a successful passivation-tethering strategy to realize tailored functional tips on the tetrapods. Such particles may be compared to the shapes and bonding functions of atoms with specific valences (colloidal atoms), and they were demonstrated to act like ‘atoms’ for self-assembled composite structures (colloidal molecules). The process of particle formation is applicable to a wide range of sol–gel materials, and the tethering can also be customized. Nanosized building blocks of even more varieties are possible by disassembling other periodic structures,<sup>36,37</sup> which may be prepared by templating<sup>38</sup> or lithographic<sup>5</sup> methods, followed by

mounting desired tethering groups. Individually, such particles with unique shapes and bonding capabilities may find applications in areas such as sensing or biomedicine<sup>39</sup> or as building blocks for proposed metanocircuits.<sup>40</sup> Collectively, they represent a general class of building blocks for experimental studies of self-assembly processes to complement simulations<sup>1,41</sup> and, in the long term, to perhaps achieve some of the highly coveted geometries for nanostructured materials.

**Acknowledgment.** This work was financially supported by the National Science Foundation (DMR-0704312). Parts of this work were carried out in the University of Minnesota Characterization Facility and Nanofabrication Center, which receive partial support from the NSF through the MRSEC, ERC, MRI, and NNIN programs. NMR instrumentation was provided with funds from the NSF (BIR-961477), the University of Minnesota Medical School, and the Minnesota Medical Foundation. The authors thank Prof. Tsapatis and Wei Fan for donating colloidal silica spheres and for assistance with dynamic light scattering experiments, and Prof. Taton and Alexi Young for taking fluorescence spectra.

**Supporting Information Available:** Additional experimental details, <sup>29</sup>Si solid-state MAS NMR spectra, TEM images of products of disassembly and coupled particles, fluorescence spectra that confirm the reactivity of the Au tips for further reaction and DLS data confirming the stability of the HS-T<sub>d</sub> and Au-T<sub>d</sub> dispersions. This material is available free of charge via the Internet at <http://pubs.acs.org>.

JA908364K

- (34) Ipe, B. I.; Shukla, A.; Lu, H.; Zou, B.; Rehage, H.; Niemeyer, C. M. *ChemPhysChem* **2006**, *7*, 1112–1118.
- (35) Nicolai, T.; Cocard, S. J. *Colloid Interface Sci.* **2001**, *244*, 51–57.
- (36) Stein, A.; Li, F.; Wang, Z. *J. Mater. Chem.* **2009**, *19*, 2102–2106.
- (37) Special issue: templated materials, *Chem. Mater.* **2008**, *20*.
- (38) Warren, S. C.; Disalvo, F. J.; Wiesner, U. *Nat. Mater.* **2007**, *6*, 156–161.
- (39) Mitragotri, S.; Lahann, J. *Nat. Mater.* **2009**, *8*, 15–23.
- (40) Engheta, N. *Science* **2007**, *317*, 1698–1702.
- (41) Hynninen, A. P.; Thijssen, J. H. J.; Vermolen, E. C. M.; Dijkstra, M.; van Blaaderen, A. *Nat. Mater.* **2007**, *6*, 202–205.